Separation Science and Technology
Publication details, including instructions for authors and subscription information:
http://www.informaworld.com/smpp/title~content=t713708471

Bacterial Alginate Role in Aerobic Granular Bio-particles Formation and Settleability Improvement

Y. M. Lin[ab]; L. Wang[a]; Z. M. Chi[b]; X. Y. Liu[a]
[a] Environmental Science and Engineering College, Ocean University of China, Qingdao, China [b] Faculty of Life Science and Technology, Ocean University of China, China

To cite this Article Lin, Y. M. , Wang, L. , Chi, Z. M. and Liu, X. Y.(2008) 'Bacterial Alginate Role in Aerobic Granular Bio-particles Formation and Settleability Improvement', Separation Science and Technology, 43: 7, 1642 — 1652
To link to this Article: DOI: 10.1080/01496390801973805
URL: http://dx.doi.org/10.1080/01496390801973805

Separation Science and Technology, 43: 1642–1652, 2008

ISSN 0149-6395 print/1520-5754 online
DOI: 10.1080/01496390801973805

Bacterial Alginate Role in Aerobic Granular Bio-particles Formation and Settleability Improvement

Y. M. Lin,[1,2] L. Wang,[1] Z. M. Chi,[2] and X. Y. Liu[1]

[1]Environmental Science and Engineering College, Ocean University of China, China
[2]Faculty of Life Science and Technology, Ocean University of China, China

Abstract: To understand the greatly enhanced settleability of aerobic granular bio-particles, bacterial alginate, one component of extracellular polysaccharides, was extracted both from aerobic granular bio-particles and the seed activated sludge. Their guluronate to mannuronate radio, reaction with Ca^{2+}, and the gel formation property were investigated and compared by the FT-Raman spectroscopy and atomic force microscopy. The larger amount of guluronate rich alginate (310 ± 16 mg g^{-1}) in the bio-particles inclines to integrate into strong gel, which becomes the structural polymer and promotes the bio-particles formation. By enlarging the particle size, increasing the density and hydrophobicity, bacterial alginate tremendously improves the granular bi-particles' setteability.

Keywords: Bio-particles, aerobic granules, bacterial alginate, settleability, biological wastewater treatment

INTRODUCTION

Activated sludge processes often suffer from inefficient settling of the microbial flocs, which always induces the deterioration in effluent quality. Recent investigations have pointed out that, aerobic granular bio-particles

Received 2 September 2007, Accepted 15 January 2008
Address correspondence to Dr. Y. M. Lin, Environmental Science and Engineering College, Ocean University of China, No. 238 Songling Road, Qingdao 266100, China. Tel./Fax: +86-532-66781819; E-mail: to_zhangmin@vip.sina.com

(AGBP) (also called aerobic granules in literatures), that are cultivated in sequence batch reactors (SBR) may have greatly enhanced settleability (1).

Some past investigations focused on the role of extracellular polysaccharides (EPS) in AGBP formation and characterization. Tay et al. found that AGBP EPS content tended to be much higher than that of sludge flocs (1). EPS contributed more to AGBP structure and stability than extracellular proteins did (2). Moreover, they shielded the bacterial cells and reduced the destruction of severe conditions toward the cells (3). To disclose EPS distribution, Chen et al. fluorescently stained their acetate-fed AGBP. Experimental results demonstrated that α and β-linked polysaccharides accumulated in their AGBP (4). The past findings affirmed the significant role of EPS on AGBP formation. Yet, it is worth noticing that EPS is only a general designation; approaches limited at this level are insufficient to reveal AGBP formation mechanism and explain their improved solid-liquid separation capacity. More information on EPS potential components, such as bacterial alginate, bacterial cellulose, etc., is required so far.

For better understanding the role of EPS in AGBP enhanced settleability, a study of the single components which can be isolated is necessary. Alginate is a family of extracellular polysaccharides produced by algae and bacteria. It consists of (1–4) linked uronic acid residues β-D-mannuronate (M) and its C-5 epimer, α-L-guluronate (G) (Fig. 1). It is believed to be a crucial constituent of activated sludge flocs. Alginate theory is one of the three theories that are currently used to explain the mechanisms of cation-induced bio-flocs formation (5).

Our hypothesis is that, alginate, due to its unique property to form gels with metal cations, could be considered as one of the main constituents of the AGBP EPS matrix. In this study, the bacterial alginates were extracted both from AGBP and the seed activated sludge (SAS), identified, characterized, and compared. The findings cast new insight on improving bio-particles' settling property and solid-liquid separation in biological wastewater treatment processes.

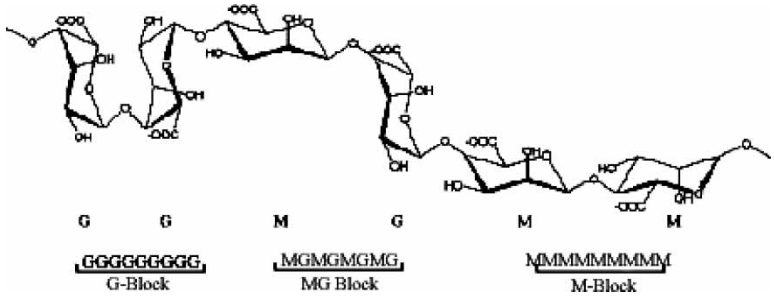

Figure 1. Alginate monomers (M: mannuronate residues, G: guluronate residues).

METHODS

AGBP Cultivation

A lab-scale SBR with a working volume of 3.6 L, an internal diameter of 6 cm and a filling height of 1.3 m was used for conducting the experiment. The reactor was operated with a cycle time of 4 h (5 min feeding, 225 min aeration, 5 min sludge settling, and 5 min for effluent withdrawal) with a volumetric exchange ratio of 50% at 25°C. The air flow rate was 3–3.5 L min^{-1}. The bioreactor was seeded with 0.5 L and returned the activated sludge from the Tuandao municipal wastewater treatment plant, Qingdao, China. Acetate was used as the sole carbon source of the synthetic wastewater with the COD loading rate of 6.0 kg m^{-3} d^{-1}. More details are specified in (1).

SAS and AGBP Parameters Measurement

The specific gravity (SG) of both SAS and AGBP were measured by the standard method (6). Their mean size was quantified by a laser particle size analysis system (Malvern Mastersizer Series 2600) and image analyzer (Quantimnet 500 Image Analyzer, Lecia Cambridge Instruments).

K, Ca, Na, Mg, Fe contents of both SAS and AGBP were determined by inductively coupled plasma (ICP, Perkin–Elmer Optima 3300 DV) after digesting 0.1 g (dry weight at 105°C) SAS and AGBP respectively with nitric acid/hydrochloric acid.

Alginate Extraction

Alginates were extracted both from SAS and AGBP according to Mchugh (7) with modifications. The biomass was washed twice with deionized water and dried at 60°C. 2 g dried biomass was extracted by 100 ml 0.2 mol L^{-1} sodium carbonate at 80°C for two hours. After dilution and filtration, the filtrate pH was adjusted to 3 by adding 0.1 mol L^{-1} H_2SO_4. After centrifugation (2000 rpm), the alginic acid precipitation was washed by deionized water until effluent pH reached 7, and dissolved in 0.1 mol L^{-1} NaOH to change into sodium alginate. Then the pH of this solution was reduced to 3 again. Those steps prevented from forming alginic acid precipitation to sodium alginate production that were formerly mentioned were repeated twice for purification. Finally we adjusted the pH of the extracted sodium alginate (ESA) solution to 7 by 0.1 mol L^{-1} H_2SO_4, and precipitated it by ethanol (50:50 (v/v)). The ESA was dried at 60°C.

ESA chemical identification and purity assay were performed according to FAO (8).

Triplicates were made in the extraction, identification, and purity assay.

ESA FT-Raman Characterization

Both ESAs were characterized by recording their FT-Raman spectra on the Raman spectrometer (Labram Infinity, France; He:Ne laser with excitation wavelength of 632.8 nm) with triplicates.

AFM Investigation on ESA-Ca^{2+} Reaction

ESA-Ca^{2+} reaction was characterized by the atomic force microscopy (AFM). Different concentrations (10, 100, 250, 500 mg L^{-1}) of both ESA_{SAS} (ESA from SAS) and ESA_{AGBP} (ESA from AGBP) were made in 40 mg L^{-1} $CaCl_2$-deionized water solution. 20 μL of each sample was deposited onto newly cleaved mica sheets for about 5 s, and then quickly removed by the pipette. Those surfaces were air dried (1 h) in a dust-free enclosure, imaged by an AFM (SPM-9500J3, SHIMADZU, Japan).

ESA-Ca Gel Formation

To test ESA-Ca gel formation property, both ESAs in 1000 mg L^{-1} deionized water solution were extruded through 20 ml syringes into 40 mg L^{-1} $CaCl_2$ deionized water solutions. The size and specific gravity of those precipitates were measured with the same methods as those of SAS and AGBP.

RESULTS

AGBP Formation and Alginate Extraction

The fluffy brown activated sludge (30–90 μm in mean size) flocs transformed to compact, round-shaped, light brown AGBP (Fig. 2a, 0.5–2 mm in

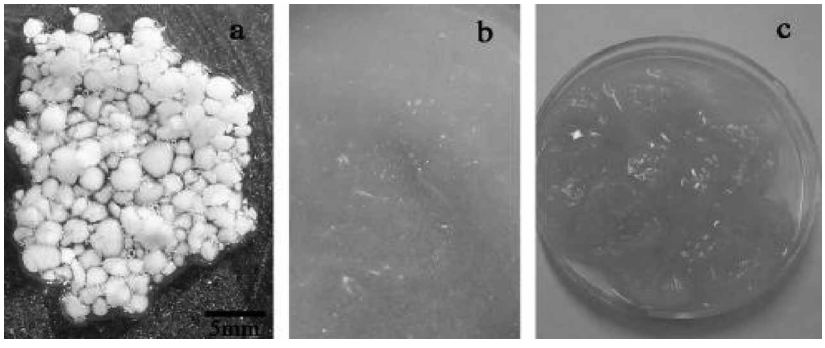

Figure 2. AGBP alginate extraction (a: AGBP, b: AGBP changed to sol in hot Na_2CO_3, c: ESA in ethanol).

diameter) after 80 days' cultivation in the SBR reactor. During alginate isolation, the AGBP disappeared in hot Na_2CO_3 and gave light yellow sol interspersed with tiny white precipitates (Fig. 2b). Soft alginic acid gel precipitates appeared when the sol pH reduced to 3. The cotton-like ESA_{AGBP} precipitated in ethanol is shown in Fig. 2c.

In contrast, during the alginate extraction of SAS, the biomass still kept their floc shape in hot Na_2CO_3 after two hours. After filtration, alginic acid gel precipitates formed in the supernatant at pH 3. ESA_{SAS} was also a cotton-like precipitation in ethanol.

Both ESAs were chemically confirmed by FAO alginate identification tests. Based on FAO purity assay, the alginate contents (expressed as $C_6H_7O_6^-$) are 139 ± 19 mg g^{-1} and 310 ± 16 mg g^{-1} for SAS and AGBP respectively. AGBP's alginate content is more than two times of SAS's.

ESA Raman Analyses

Alginate refers to a family of linear polysaccharides containing 1,4 linked β-D-mannuronate (M) and α-L-guluronate (G) acid residues. Those residues typically occur as $(\text{-M-})_n$, $(\text{-G-})_n$ and $(\text{-MG-})_n$ blocks (Fig. 1). M- and G-blocks display significantly different structures, and their proportion in the alginate (G/M ratio) determines the diversity of physicochemical properties and reactivity of these polysaccharides (9). Raman spectroscopy is believed to provide the information for the alginate G/M ratio (10, 11). The presence of these two residues can be identified from their characteristic Raman peaks: M at 1100 cm^{-1}, while G at 1025 cm^{-1}. The G/M ratio can be calculated from the intensities of these two peaks (11). The G/M ratios obtained from their characteristic Raman peaks are 0.94 and 1.18 for ESA_{SAS} and ESA_{AGBP} respectively, which demonstrates that, more G-blocks are present in the alginate after AGBP formed (Figure 3).

AFM Investigation on ESA-Ca^{2+} Reaction

The major metal ions existed in the synthetic wastewater during AGBP cultivation are Ca^{2+}, Mg^{2+}, K^+, Na^+, Fe^{3+}, their contents in AGBP are listed in Table 1. Same measurements were also performed for SAS as the comparison. Ca is found to be the most abundant metal component in both SAS and AGBP.

Since the unique property of alginate is its ability to react with polyvalent metal cations (except Mg^{2+}) to produce gels under mild conditions (12), considering the abundance of Ca in both SAS and AGBP, ESA-Ca^{2+} reactions were investigated by AFM. A completely different aggregating tendency was found between ESA_{SAS}-Ca^{2+} and ESA_{AGBP}-Ca^{2+} (Figure 4).

ESA_{AGBP} transferred from randomly distributed globules, to a rod-like and a flower-shaped aggregations, and finally to an ordered weblike network

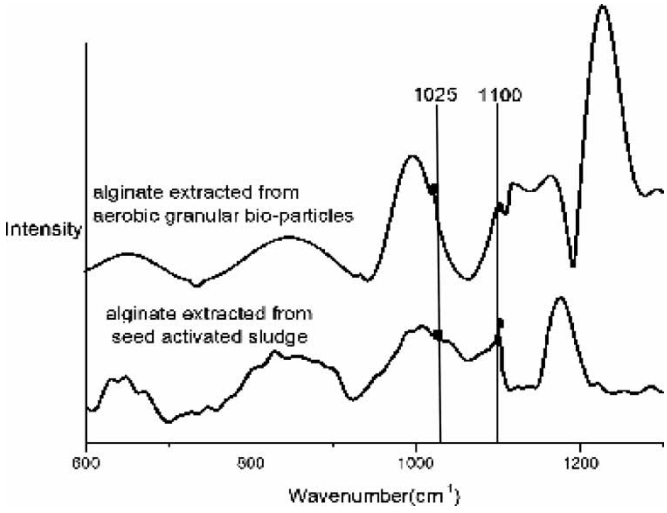

Figure 3. Raman spectra of ESA_{AGBP} and ESA_{SAS}.

(Figs. 4a–4d), as its concentrations increased from 10 mg L^{-1} to 500 mg L^{-1} in 40 mg L^{-1} $CaCl_2$ solution. It seems that, with raised concentrations, ESA_{AGBP} molecules tend to combine together forming tri-dimensional aggregations with enlarged particle size, when they react with $CaCl_2$ (the strip at the lower part of each photo in Fig. 4 demonstrates the aggregate altitude).

This phenomenon of alginate molecules' self-integration is called molecular self-assembly (13), which relies on the strong interactions between Ca^{2+} ions and G-blocks. Due to M and G monomers' particular shapes and their modes of linkage respectively, the geometries of G-block, M-block, and MG block are substantially different. Specifically, the G-blocks are buckled while the M-blocks are flat ribbon-like (Fig. 1). If two G-blocks are aligned side by side, diamond shaped holes result (Fig. 4f). Their dimensions are ideal for the cooperative binding of Ca^{2+}ions (and

Table 1. Ca, Mg, K, Na, Fe contents in seed activated sludge (SAS) and aerobic granular bio-particles (AGBP)

Mg g^{-1}	Seed activated sludge	Aerobic granular bio-particles
Ca	18.4 ± 0.3	57.7 ± 0.5
Mg	2.17 ± 0.16	0.713 ± 0.008
K	4.92 ± 0.35	0.187 ± 0.001
Na	2.58 ± 0.43	25.4 ± 0.3
Fe	0.492 ± 0.005	0.308 ± 0.002

other polyvalent metal ions) (9). The GG-Ca region is insoluble. Thus, when ESA_{AGBP} mixes with $CaCl_2$ solution, the insoluable GG-Ca quickly forms the core surrounded by M and MG blocks under the repulsion of water molecules. The Ca^{2+} localizing in the immediate vicinity of COO^- in M and MG blocks partially neutralize the electrostatic repulsion among COO^-, which results in the globule formation (Fig. 4a). As ESA_{AGBP} concentration increases, more chances are brought forth for Ca^{2+} ions to complex with G blocks from different molecular chains due to ESA_{AGBP}'s higher G contents. Combining with the effect of alginate intermolecular hydrogen bonds, the rod-like ESA_{AGBP} condensations are produced (Fig. 4b). Consequently, globules and rods assembled the flower-shaped condensations (Fig. 4c), and finally the ordered tri-dimensional networks (Fig. 4d). This phenomenon of transferring from disorder to order is driven by calcium-induced association of G-blocks. G-block abundance is determined if Ca^{2+} ions are sufficient (13). Therefore, it is ESA_{AGBP}'s higher G/M ratio that brings more chances for Ca^{2+} to integrate G-blocks from different alginate chains, and detrimentally decides the strong network formation.

In contrast, as ESA_{SAS} concentration increased, only tiny flocs formed. Although globules and rods are also the basic "bricks" for these flocs (magnification in Fig. 4e), no interconnection happened among flocs. When the concentration reached 500 mg L^{-1}, the diameter of those flocs was 0.5–2 μm (Fig. 4e), which is significantly different from the integrated ESA_{AGBP}-Ca

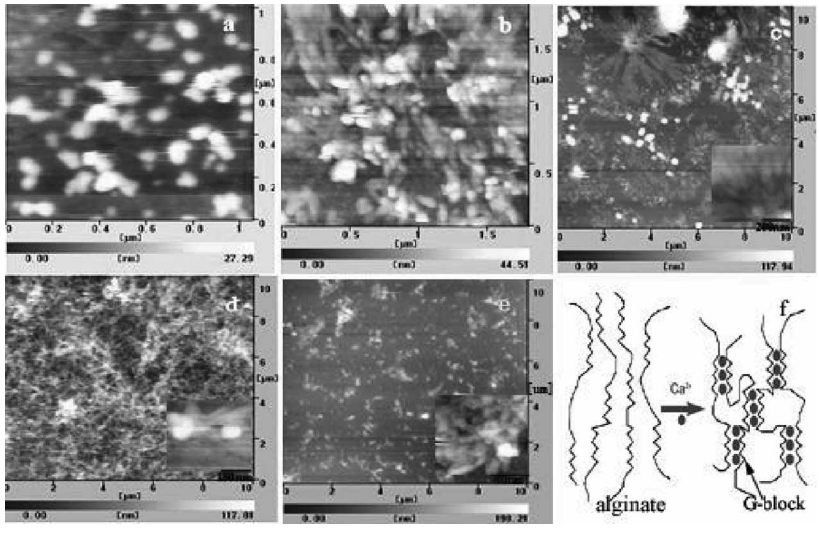

Figure 4. ESA-Ca^{2+} reactions with increased ESA concentrations under atomic force microscopy (AFM). a–d: ESA_{AGBP}-Ca^{2+} reactions with ESA_{AGBP} concentrations increased from 10, 100, 250, to 500 mg L^{-1}; e: ESA_{SAS}-Ca^{2+} reaction with ESA_{SAS} concentration of 500 mg L^{-1}; f: Ca^{2+} induced G-block association.

tri-dimensional network with the mean size larger than 10 μm at the same concentration (Fig. 4d). This difference probably attributes to ESA_{SAS}' lower G/M ratio. Inadequate G-blocks are provided for the inter-chain dimerization with Ca^{2+}, which inhibits ESA_{SAS}' further integration.

Alginate-Ca Gel Formation

Once ESA_{AGBP} drops contacted with $CaCl_2$ solution after being extruded from the syringe, granules with the same diameter as those drops formed and settled down. Comparatively, the ESA_{SAS} drops dispersed into tiny flocs in $CaCl_2$ and suspended (Fig. 5). Their specific gravity and sizes are listed in Table 2. With larger numbers of G-blocks crosslink Ca^{2+}, ESA_{AGBP} molecules are able to hold the drop size as Ca^{2+} penetrating from its border into the core. While ESA_{SAS} molecules are not powerful enough due to their low G/M ratio, only smaller size of flocs sustain by GG-Ca^{2+} binding. Apparently, the compact ESA_{AGBP}-Ca granules hold tremendously great numbers of alginate molecules than the fluffy ESA_{SAS}-Ca flocs, which contributes to ESA_{AGBP}-Ca granules' higher specific gravity. In addition, it is observed that ESA-Ca takes on the shape as their original biomass respectively. Although it is incomparable between the sizes and densities of ESA-Ca aggregations and those biomass (Table 2), information still could be deducted that, bacterial alginate is the structural polymer of AGBP. It has great influence on AGBP characteristics, from their shape to their properties.

DISCUSSION

Alginate Role on AGBP Formation

After AGBP's formation, biomass alginate content increased from 139 ± 19 mg g^{-1} of seed activated sludge to 310 ± 16 mg g^{-1}; alginate's

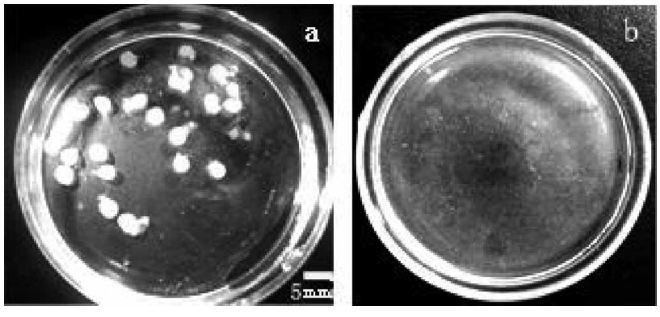

Figure 5. ESA-Ca gel formations. a: ESA_{AGBP}-Ca; b: ESA_{SAS}-Ca.

Table 2. Specific gravity and size data of seed activated sludge, aerobic granular bioparticles, ESA_{AGBP}-Ca granules and ESA_{SAS}-Ca flocs

	Seed activated sludge	Aerobic granular bioparticles	ESA_{AGBP}-Ca granules	ESA_{SAS}-Ca flocs
Specific gravity	1.002 ± 0.002	1.036 ± 0.011	1.124 ± 0.006	0.092 ± 0.0014
Size (mm)	0.068 ± 0.009	1.7 ± 0.5	2.3 ± 0.4	0.015 ± 0.004

G/M ratio changed from 0.94 to 1.18. Larger amount of alginate with higher G content presents in AGBP. ESA_{AGBP} molecules have the inclination of self-assembly under the inducement of Ca^{2+}. Their molecular interconnection property results in the ESA_{AGBP}-Ca granules formation.

Bacterial alginate is a family of extracellular polysaccharides secreted by certain bacterial species under nutrient deficient conditions. Their formation and properties (e.g. G/M ratio) are decided by some enzymes, whose secretions are triggered by the environmental conditions (14). Till now, almost all AGBP were cultivated in the SBR. The unique feature of a SBR is its cyclic operation, which leads to the periodical biodegradation phase followed by the aerobic starvation phase in every cycle (2). These food shortage phases, together with those strong selective pressure from the specific reactor operational conditions as short settling time, high reactor H/D ratio (the ratio of reactor height to diameter), and high shear force etc. (2), promote the secretion of bacterial alginate with certain molecular properties. By the reactions with polyvalent metal ions, alginate-metal gels accumulate in the reactor. This naturally formed network matrix offers microorganisms the same inhabitancy and protection as the manmade immobilizations do. On the other hand, by the chemical and physical combinations between alginates' active functional groups (-COO^-, -OH etc.) and other extracellular polysaccharides species and proteins, more extracellular polymers aggregate on these gels. Therefore, with alginate-metal gel as the structure polymer, the complex aerobic granular bio-particles form as the result of the joint efforts of all the extracellular polymers.

Alginate Role on AGBP Enhanced Settleability

As demonstrated by AFM investigation, ESA_{AGBP} tends to form aggregations with enlarged particle size (from 70 nm to more than 10 μm in Fig. 4) at locally increased concentrations under the inducement of Ca^{2+}. ESA_{AGBP}-Ca's compact structure contributes to its larger alginate amount per unit space than the fluffy ESA_{SAS}-Ca floc, which results to its higher density. Therefore, alginate's accumulation in AGBP both increases the size and the density. According to the stock's law, the greatly increased particle size and

density significantly accelerate the settling velocity and improve the setteability.

$$v_P = \frac{g(\rho_p - \rho_w)d_p^2}{18\mu} \tag{1}$$

Additionally, ESA_{AGBP}'s higher G/M ratio reflects that larger numbers of G-blocks exist in AGBP, which complex with polyvalent metal cations form insoluble regions. This may increase AGBP's hydrophobicity, make AGBP easily separate from water.

Therefore, bacterial alginate accumulated in AGBP tremendously improve their settling property by enlarging the particle size, increasing the density and hydrophobicity.

CONCLUSIONS

Bacterial alginate, the extracellular polysaccharides secreted by bacteria, accumulated in aerobic granular bio-particles with the content of 310 ± 16 mg g^{-1}. Characterized by its G/M ratio of 1.18, this G-block rich bacterial alginate tended to integrate into an ordered network with an enlarged size under the inducement of Ca^{2+}, and easily formed alginate-Ca granules. The naturally formed alginate-metal gel matrix promotes AGBP formation by providing for the structural polymer. By enlarging the particle size, increasing the density and hydrophobicity, bacterial alginate in AGBP improves their setteability. The study will bring new insight on improving solid-liquid separation in biological wastewater treatment processes.

NOMENCLATURE

v_p	particle settling velocity, m s^{-1}
d_p	diameter of particle size, m
μ	dynamic viscosity, N s m^{-1}
ρ_w	density of water, kg m^{-3}
ρ_p	density of particle, kg m^{-3}
g	acceleration due to gravity, 9.81 m s^{-2}

ACKNOWLEDGMENTS

This work was supported by the China National Foundation for Natural Science No. 30570339. Authors would like to thank Professor Avner Adin (Israel) for his helpful suggestions.

REFERENCES

1. Tay, J.H., Liu, Q.S., and Liu, Y. (2001) Microscopic observation of aerobic granulation in sequential aerobic sludge blanket reactor. *J. Appl. Microbiol.*, 91: 168.
2. Liu, Y.Q., Liu, Y., and Tay, J.H. (2004) The effects of extracellular polymeric substances on the formation and stability of biogranules. *Appl. Microbiol. Biotechnol.*, 65: 143.
3. Wang, L. and Lin, Y.M. (2007) Spore detection in aerobic granules by different dipicolinic acid. *Bioresour. Technol.*, 98: 3164.
4. Chen, M.Y., Lee, D.J., and Tay, J.H. (2007) Distribution of extracellular polymeric substances in aerobic granules. *Appl. Microbiol. Biotechnol.*, 73: 1463.
5. Sobeck, D.C. and Higgins, M.J. (2002) Examination of three theories for mechanisms of cation-induced biofloculation. *Water Research*, 36: 527.
6. APHA. (1998) *Standard Methods for the Examination of Water and Wastewater*, 20th edn.; American Public Health Association: Washington, DC.
7. Mchugh, D.J. (2003) *A Guide to the Seaweed Industry*. FAO Fisheries Technical Paper 441. FAO of the United Nations, Room.
8. FAO. (1997) "Compendium of food additive specifications. Addendum 5". (FAO Food and Nutrition Paper-52 add. 5) Joint FAO/WHO Expert Committee on Food Additives 49th session, Rome.
9. Davis, T.A., Volesky, B., and Mucci, A. (2003) A review of the biochemistry of heavy metal biosorption by brown algae. *Water Research*, 37: 4311.
10. Salomonsen, T., Jensen, H.M., Stenbæk, D., and Engelsen, S.B. (2008) Chemometric prediction of alginate monomer composition. A comparative spectroscopic study using IR, Raman, NIR and NMR. *Carbohydrate Polymers*, CARBPOL-D-07-00446.
11. Pereira, L., Sousa, A., Coelho, H., Amado, A.M., and Ribeiro-Claro, P.J.A. (2003) Use of FTIR, FT-Raman and ^{13}C NMR spectroscopy for identification of some seaweed phycocolloids. *Biomolecular Engineering*, 20: 223.
12. Grant, G.T., Morris, E.R., Rees, D.A., Smith, P.J.C., and Thom, D. (1973) Biological interactions between polysaccharides and divalent cations: the egg-box model. *Febs. Letters*, 32: 195.
13. Jiang, M., Eisenberg, A., Liu, G.J., and Zhang, X. (2006) *Macromolecular Self-assembly*, 1st edn.; Science Publication: Beijing, China.
14. Sutherland, I.W. (2001) Microbial polysaccharides from Gram-negative bacteria. *International Dairy Journal*, 11: 663.